Libyan Journal of Ecological & Environmental Sciences and Technology
(LJEEST)

LJEEST
ISSN: 2710-5237
www.srcest.org.ly/jou

http://aif-doi.org/LJEEST/060206

MEMBRANE-BASED CARBON DIOXIDE CAPTURE FROM AIR: PERFORMANCE EVALUATION AND ENERGY CONSIDERATIONS IN COMPLETE MIXING AND CROSSFLOW MODELS

Mawaheb Mohamed Zarok Derdar[1], and Heba Ali Sadegh Elhouni[1]

ARTICLE INFO

Vol. 6 No. 2 Dec, 2024
Pages (34- 42)

Article history:
Revised form 28 August 2024
Accepted 29 November 2024

Authors affiliation
Faculty of Engineering, University of Tripoli, Tripoli, Libya.

m.derdar@uot.edu.ly

Keywords:
Membrane; Direct air capture; Carbon dioxide removal

ABSTRACT

This study investigates the utilization of membrane processes for the direct capture of carbon dioxide (CO_2) from air, a technology of increasing interest for reducing greenhouse gas emissions. However, its adoption remains controversial within the engineering community due to the high dilution level of CO_2 in air. The research focuses on evaluating the separation performance of a membrane unit for CO_2 capture from air, taking into account the influence of membrane material properties and operating conditions on energy requirements. The models considered in this paper are complete mixing and crossflow models. As for the methods used for estimating both models are Excel Sheet and Polymath Software, respectively. The findings indicate that membranes necessitate either high selectivity and carbon dioxide permeance or a lower pressure ratio (permeate to feed pressure) to achieve higher purity in a single stage. When comparing the mole fraction of carbon dioxide in the permeate side at the crossflow model, the results exhibit an 8.2% percent error compared to the literature value of 6000 ppm. The study provides insights into the capabilities and limitations of membrane technology for direct CO_2 capture from air. However, from a practical standpoint, the achievable CO_2 purity level (5506ppm) may be deemed insufficient for various target applications.

استخراج ثاني أكسيد الكربون من الهواء باستخدام تقنية الغشاء: تقييم الأداء واعتبارات الطاقة في حالتي الخلط الكامل والتدفق المتقاطع.

مواهب الزروق الدردار   هبة علي الصادق الهوني

تستكشف هذه الدراسة استخدام عمليات الغشاء لاستخراج ثاني أكسيد الكربون مباشرة من الهواء، وهي تقنية أثارت اهتماً ما متزايدًا للحد من انبعاثات غازات الاحتباس الحراري، ولكنها لا تزال مثيرة للجدل بين مجتمع الهندسة بسبب التركيز القليل لثاني أكسيد الكربون في الهواء. تتحقق الدراسة من أداء وحدة الغشاء لاستخراج ثاني أكسيد الكربون من الهواء، مع النظر في دور أداء المواد الغشائية وتأثير ظروف التشغيل على الطاقة المطلوبة باستخدام نماذج المزج الكامل والتدفق المتقاطع. تشير النتائج إلى أن الغشاء يتطلب اما انتقائية عالية ونفاذية ثاني أكسيد الكربون أو نسبة ضغط أقل (ضغط النافذ إلى ضغط الداخل) لتحقيق نقاء أعلى في مرحلة واحدة. بالنسبة للكسر المولي لثاني أكسيد الكربون في النافذ في نموذج التدفق المتقاطع، تعطي النتائج خطأ نسبته 8.2% مقارنة بالمراجع (6000 جزء في المليون). توفر الدراسة إرشادات حول إمكانيات وقيود الغشاء لاستخراج ثاني أكسيد الكربون مباشرة من الهواء. من وجهة نظر عملية، يمكن توقع أن مستوى نقاء ثاني أكسيد الكربون المتحصل عليها (5506 جزء في المليون) أن يكون منخفضا جدًا لعدة تطبيقات مستهدفة.

INTRODUCTION

The escalating issue of global warming caused by greenhouse gas emissions, particularly carbon dioxide (CO_2), poses significant challenges to our environment and society. The Intergovernmental Panel on Climate Change (IPCC) has expressed growing concerns about the rising CO_2 concentration in the atmosphere and its adverse effects on climate patterns, sea levels, and ecosystems (Sandalow et al. 2018). Despite international efforts, such as the Paris Agreement, progress in reducing emissions has been insufficient to mitigate these risks effectively. Therefore, exploring additional strategies for CO_2 removal, such as Carbon Dioxide Removal (CDR) technologies, is crucial.

Carbon Dioxide Removal Technologies:

CDR technologies encompass various methods for extracting CO_2 from the atmosphere. These methods can be broadly classified into natural, technological, and hybrid pathways. Natural approaches include afforestation and reforestation, which utilize the ability of plants to absorb CO_2 through photosynthesis. Technological methods involve direct capture of CO_2 from ambient air, such as Bioenergy with Carbon Capture and Storage (BECCS) and Direct Air Capture (DAC). Hybrid pathways combine natural and technological methods to achieve CO_2 removal.

Direct Air Capture Technologies

Direct Air Capture Overview. Direct Air Capture (DAC) is a promising approach for CO_2 removal from the atmosphere. It involves physically or chemically extracting CO_2 directly from ambient air, which can then be utilized for various purposes, including storage, industrial applications, or utilization in the production of fuels and chemicals. DAC technologies have the potential to contribute significantly to global climate mitigation efforts, particularly in achieving net-negative emissions.

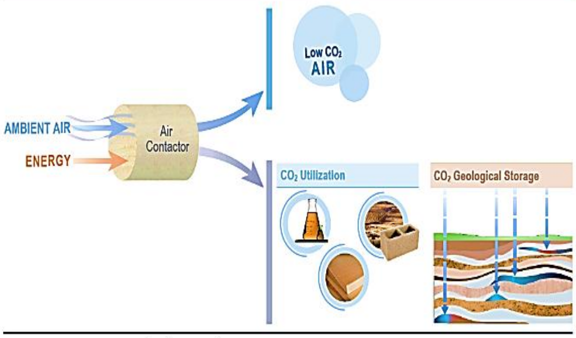

Fig. (1): Direct Air Capture of Carbon Dioxide

Membrane-Based Direct Air Capture

Among the various DAC methods, membrane-based separation has gained attention due to its low energy requirements and potential for large-scale deployment. Membrane-based DAC utilizes different membrane materials and separation mechanisms, such as gas permeation, gas diffusion in a porous solid, ionic exchange, and reverse osmosis, to selectively capture CO_2 from air. This study focuses on analyzing the performance of membrane units for CO_2 capture, considering both single-stage and multistage configurations.

The objective of this study is to investigate the separation performances of membrane units for CO_2 capture from air. Specifically, the study aims to analyze the impact of membrane material performances, including permeances and selectivity, as well as operating conditions, on energy requirements. Both complete mixing and crossflow models will be employed to evaluate the efficiency and feasibility of membrane-based CO_2 capture technologies. The findings of this study will contribute to the understanding of the potential of membrane-based separation for large-scale CO_2 removal from the atmosphere.

In summary, this paper presents a comprehensive study on membrane-based CO_2 capture technology from an engineering design perspective. The investigation focuses on the separation performances of single and multistage membrane units and their energy requirements. The results of this study will provide valuable insights into the feasibility and potential of membrane-based DAC for large-scale CO_2 removal, contributing to the advancement of carbon capture and climate mitigation strategies.

Materials and Methods

The procedures for this study involved the use of membrane processes for direct capture of carbon dioxide (CO_2) from air. The study design aimed to evaluate the separation performance of a membrane unit for a single stage and multistage for CO_2 capture, considering membrane material properties and the impact of operating conditions on energy requirements assuming complete mixing and crossflow models.

Important operating conditions for membrane-based direct air capture (m-DAC) have been established by (Fujikawa et al, 2021). using chemical process simulation. These conditions encompass a retentate CO_2 concentration of 300 ppm, a feed pressure of 101.3 kPa (1 atm), a permeate vacuum of 5 kPa, and a multistage separation approach to attain the desired CO_2 concentration in the permeate (0.6% for the first stage). Apart from the intrinsic membrane properties, such as permeance and selectivity, process design parameters including operation pressures, permeate composition, and stage cut (the fraction of feed gas passing through the membrane) are also vital considerations.

Complete-Mixing Model for Gas Separation by Membranes

Figure (2) presents a process flow diagram that assumes complete mixing, depicting the operational concept. In cases where the separator element operates at a low recovery rate, meaning that the permeate flow rate is significantly smaller than the feed rate, there is minimal alteration in composition. Hence, the complete-mixing model provides a reasonable approach to estimate permeate purity under such conditions. This conclusion was derived by Weller and Steiner (1993)

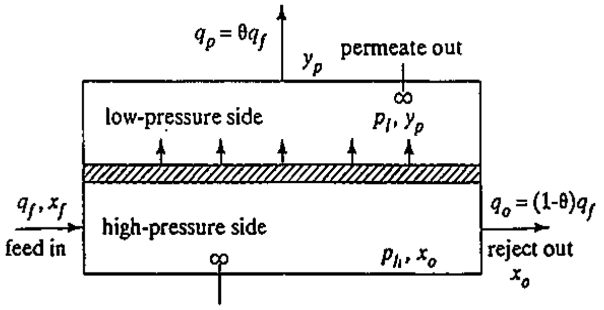

Figure (2): Process Flow for Complete Mixing

the rate of diffusion or permeation of CO_2 is given by Equation (1) below:

$$\frac{q_p . y_p}{A_m} = \frac{P'_{CO_2}}{t}(p_h . x_o - p_l . y_p) \qquad (1)$$

For a binary system the other gas say nitrogen rate of diffusion is presented as follows

$$\frac{q_p(1-y_p)}{A_m} = \frac{P'_{N_2}}{t}(p_h(1 - x_o) - p_l(1 - y_p)) \qquad (2)$$

Where P'_{N_2} is the permeability of nitrogen. dividing Eq (1) by (2) to get:

$$\frac{y_p}{1-y_p} = \frac{\alpha\left[x_o - \left(\frac{p_l}{p_h}\right)y_p\right]}{(1-x_o) - \left(\frac{p_l}{p_h}\right)(1-y_p)} \qquad (3)$$

Equation (3) is a quadratic equation, and its solution is:

$$y_p = \frac{-b + (b^2 - 4ac)^{0.5}}{2a} \qquad (4)$$

where $a = 1 - \alpha$, $b = \frac{p_h}{p_l}(1 - x_o) - 1 + \alpha\frac{p_h}{p_l}x_o + \alpha$, $c = -\alpha\frac{p_h}{p_l}x_o$

Hence, upon estimating the value of y_p, it is substituted into the component material balance equation to determine the stage cut. Subsequently, the membrane area is calculated using the rate of diffusion Equation (1)

2.2 Complete-Mixing Model for Multicomponent Mixtures

The process flow diagram, as depicted in Figure (2), illustrates the feed composition x_f, represented by is x_{fA}, x_{fB}, x_{fC}, and x_{fD}. In terms of volume, Earth's atmosphere comprises approximately 78.08 percent nitrogen, 20.95 percent oxygen, 0.93 percent argon, and 0.04 percent carbon dioxide [4]. The known parameters in this study include the feed composition, membrane permeance, feed and permeate pressures, outlet reject CO_2 mole fraction, and selectivity of other gases (CO_2/X).

The values to be determined in this study include the stage cut, permeate composition, retentate or reject composition of other gases, and the required membrane area. These unknowns are obtained by solving a set of simultaneous equations using the iteration method.

The rate of permeation equations, similar to Equation (1) can be expressed as follows:

$$q_p . y_{pi} = \frac{P'_i}{t}A_m(p_h . x_{oi} - p_l . y_{pi}) \qquad (5)$$

where i stands for (CO_2, O_2, N_2, Ar)

material balance equations:

$$q_f . x_{fi} = q_p . y_{pi} + q_o . x_{oi} \qquad (6)$$

dividing Eq (6) by q_f and solving for the outlet reject composition:

$$x_{oi} = \frac{1}{1-\theta}x_{fi} - \frac{\theta}{1-\theta}y_{pi} \qquad (7)$$

and for y_{pi}:

$$y_{pi} = \frac{x_{fi} - (1-\theta)x_{oi}}{\theta} \qquad (8)$$

also, two final equations can be written as:

$$\textstyle\sum_i^n y_{pi} = 1 \qquad (9)$$

$$\textstyle\sum_i^n x_{oi} = 1 \qquad (10)$$

Rearranging Eq (5) and solving for A_m:

$$A_m = \frac{q_p . y_{pi} . t}{P'_i[p_h . x_{oi} - p_l . y_{pi}]} \qquad (11)$$

Rearranging Eq (11) for y_{pi} and substituting x_{oi} value from Eq (7)

$$y_{pi} = \frac{p_h . x_{fi}/(1-\theta)}{q_p . \frac{t}{P'_i . A_m} + \frac{\theta p_h}{1-\theta} + p_l} \qquad (12)$$

Iteration Solution Procedure for Multicomponent Mixtures

The following iterative or trial-and-error procedure can be employed to solve the aforementioned equations:

1. Assume a value of θ, where $0 < \theta < 1$.
2. Utilizing Equation (8), calculate the retentate mole fraction of CO_2 (x_o), and determine y_p for CO_2, using the assumed value of θ.
3. Calculate the membrane area using Equation (11).
4. Determine the values of $y_{pi}$for other gases, using Equation (12) with the calculated value of A_m from step 3.
5. Calculate the sum Σy_{pi}. If the sum is not equal to 1.0, repeat steps 1 through 5 until the sum reaches 1.0.
6. Finally, calculate the x_{oi} values for other gases using Equation (7).

Crossflow Model for Gas Separation by Membranes

According to this model, there is no mixing on the high-pressure side or the permeate side. Consequently, the permeate composition at any given point along the membrane is determined by the relative permeation rates of the different components of the feed at that particular point.

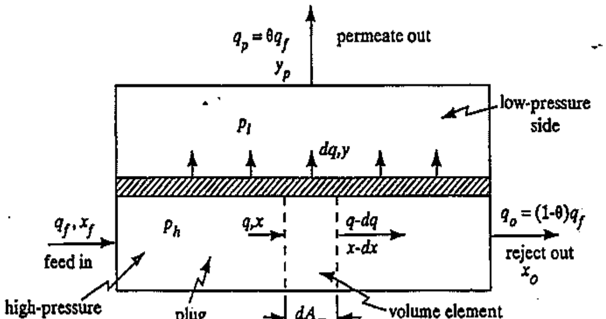

Figure (3): Process Flow Diagram for Crossflow

The local permeation rate over a differential membrane area dA_m at any point in the stage is

$$y.dq = \frac{P'_{CO_2}}{t}[p_h.x - p_l.y].dA_m \qquad (13)$$

$$(1-y).dq = \frac{P'_{N_2}}{t}[p_h.(1-x) - p_l.(1-y)].dA_m \qquad (14)$$

where dq is the total flow permeating through the area dA_m. Dividing Eq. (13) by (14) gives

$$\frac{y}{1-y} = \frac{\alpha\left[x-\left(\frac{p_l}{p_h}\right)y\right]}{(1-x)-\left(\frac{p_l}{p_h}\right)(1-y)} \qquad (15)$$

This equation establishes a relationship between the permeate composition y and the reject composition x at a specific point along the path. It bears resemblance to Equation (3) for complete mixing. Weller and Steiner employed clever transformations and successfully derived an analytical solution for the three equations, as follows:

$$\frac{(1-\theta^*)(1-x)}{1-x_f} = \left(\frac{u_f-\frac{E}{D}}{u-\frac{E}{D}}\right)^R \left(\frac{u_f-\alpha+F}{u-\alpha+F}\right)^S \left(\frac{u_f-F}{u-F}\right)^T \qquad (16)$$

Where,

$$\theta^* = 1-\frac{q}{q_f}, i = \frac{x}{1-x}, \ u = -Di + (D^2i^2 + 2Ei + F^2)^{0.5}$$

$$, D = 0.5[\frac{(1-\alpha)p_l}{p_h} + \alpha] \ .E = \frac{\alpha}{2} - DF,$$

$$F = -0.5[\frac{(1-\alpha)p_l}{p_h} - 1], R = \frac{1}{2D-1}, S = \frac{\alpha(D-1)+F}{(2D-1)\left(\frac{\alpha}{2}-F\right)},$$

$$T = \frac{1}{1-D-\frac{E}{F}}$$

The term u_f represents the value of u at $i = i_f = x_f/(1-x_f)$.The value of θ^* corresponds to the fraction permeated up to the value of x in Figure (3). At the outlet, where $x = x_o$, θ^* is equal to θ, representing the total fraction permeated. The composition of the exit permeate stream is denoted as y_p and is calculated using the material balance equation, Eq (8).

Similar to Equation (4), the quadric equation (15) is solved to obtain the solution:

$$y = \frac{-b+(b^2-4ac)^{0.5}}{2a} \qquad (17)$$

where, $a = 1-\alpha$, $b = -1+\alpha+\frac{1}{r}+\frac{x}{r}(\alpha-1)$,

$c = -\frac{\alpha x}{r}$

Equation (17) holds significant value in the Algebraic-differential equations employed to solve the crossflow model. In addition to that, the ordinary differential equations used in the model are as follows [5].

$$\frac{dq}{ds} = -\sum_{i=1}^{n} J_i(x_i, y_i, p_l, p_h) \qquad (18)$$

$$\frac{dx_i}{ds} = \frac{x_i\sum_{i=1}^{n} J_i(x_i,y_i,p_l,p_h) - J_i(x_i,y_i,p_l,p_h)}{q} \qquad (19)$$

$$J_i = \frac{P'_i}{t}(x_i.p_h - y_i.p_l) \qquad (20)$$

where,

$\frac{P'_i}{t} = \frac{\text{permibility}}{\text{thickness}} = \frac{\text{Barrer}}{\mu m} = \text{GPU} = \text{Gas Permeance}$, S is the membrane area, and q is the flow in the upstream which varies from q_f to q_o, boundary conditions are:

at $S = 0$, $q = q_f$, $x_I = x_f$ and at $S = A_m$, $q = q_o$,

$x_i = x_o$

This set of ordinary differential equations (ODEs), along with Eq (17), is input into the Polymath software to solve them using the Runge-Kutta-Fehlberg Method (RKF45). It is assumed that the system is binary.

Furthermore, the investigation of feed compression and/or vacuum pumping allows for the determination of energy requirements (E), which can be obtained using the following expressions (Castel et al. 2021). The adiabatic expansion coefficient of the gas mixture (γ), representing the ratio of pressure over volume heat capacity, is assumed to be 1.4 for air (Cengel 2009). The ideal gas constant (R) is equal to 8.314 J/gmol·K (Smith et al. 2022), and T represents the temperature in Kelvin at standard conditions.

$$E_{vacuum} = \frac{\gamma.RT}{y(\gamma-1)}\left(\left(\frac{p_{atm}}{p_l}\right)^{\frac{\gamma-1}{\gamma}} - 1\right) \qquad (21)$$

From a thermodynamic perspective (Castro et al. 2022), the low concentration of CO_2 in the feed plays a significant role. The minimum work (W_{min}) under isothermal conditions can be determined using Equation (22).

$$W_{min} = RTln\left(\frac{p_l}{p_h}\right) \qquad (22)$$

RESULTS AND DISCUSSION

Membrane Condition of 40,000 GPU for Complete Mixing Flow Case in Multicomponent and Binary Systems.

Table (1): The First Conditions of 40,000 GPU Assuming Basis of Feed Equals 1 m³/s.

x_f	x_o	q_f (m^3/s)	p_l (kpa
0.0004	0.0003	1	5
p_h (kpa)	P_{CO_2}(GPU)	α	r (p_l/p_h
101	40,000	70	0.0495

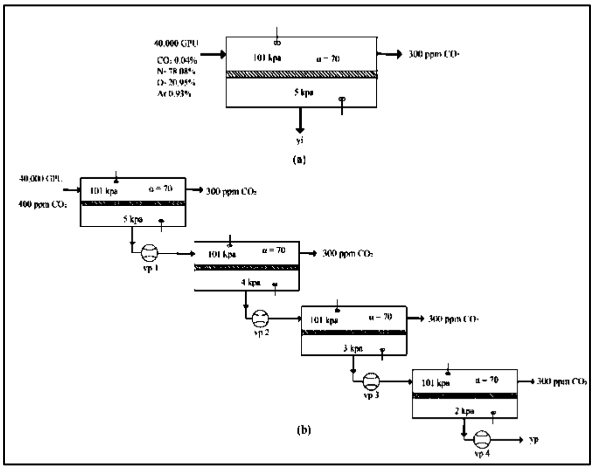

Figure (4): Process Flow Diagram for Complete Mixing Model 40,000 GPU, a) Multicomponent System Single Stage, b) Binary System Multistage.

Table (1) displays the chosen conditions for the feed and permeate mole fractions, along with the assumed feed rate of 1 m³/s. On the other hand, Figure (4) illustrates two scenarios: (a) a single-stage multicomponent system, and (b) a multistage binary system.

Table (2): The Results of Permeate Mole Fraction and Area for Multicomponent System

	x_f	y_i	x_o
CO_2	0.0004	0.00475	0.0003
N_2	0.7808	0.77740	0.7809
O_2	0.2095	0.20859	0.2095
Ar	0.0093	0.00926	0.0093
sum	1.00000	1.00000	1.00000

θ	y_p	q_p (m^3/s)	A_m (m^2)	R_c
0.02247	0.00475	0.022468	54.353	0.266851

The values reported in Table (2) were estimated using an Excel sheet solver. The solver was employed to solve the equations for the mole fractions of the four components by iteratively adjusting the stage cut value until the summation of mole fractions on the permeate side reached unity.

Table (3): Vacuum Pump Required Energy for Multicomponent

γ (25 C)	1.4
R (J/gmol. k)	8.314
T (k)	298
E_{vacuum} (KJ)	2482.825
W_{min} (KJ)	-7.4468

Table (4): Permeate Mole Fraction of CO_2 and Membrane Area for Binary System Multistage.

stage	1	2	3	4
p_l (kpa)	5	4	3	2
r (p_l/p_h)	0.05	0.04	0.03	0.02
y_p	0.004714	0.0056	0.0068	0.0088
θ	0.022655	0.833	0.815	0.765
A_m (m^2)	53	44.6	35.2	27.17
E_{vacuum} (KJ)	2502.204	2346.921	2207.577	2036.406

Upon reviewing the results presented in Table (2) to Table (4) for both multicomponent and binary systems, it is evident that the disparities in the permeate mole fraction, stage cut, and required membrane area are negligible. Therefore, for the sake of simplification, the multistage system is approximated as a binary system by adjusting the pressure ratio to achieve the desired retentate mole fraction.

3.2 Membrane Condition of 10,000 GPU for Complete Mixing Flow Case in Multicomponent and Binary Systems

Table (5): The Second Conditions of 10,000 GPU

x_f	x_o	q_f (m^3/s)	p_l (kpa)
0.0004	0.0003	1	2
P_{CO_2} (GPU)	p_h (kpa)	α	r (p_l/p_h)
10,000	110	30	0.018182

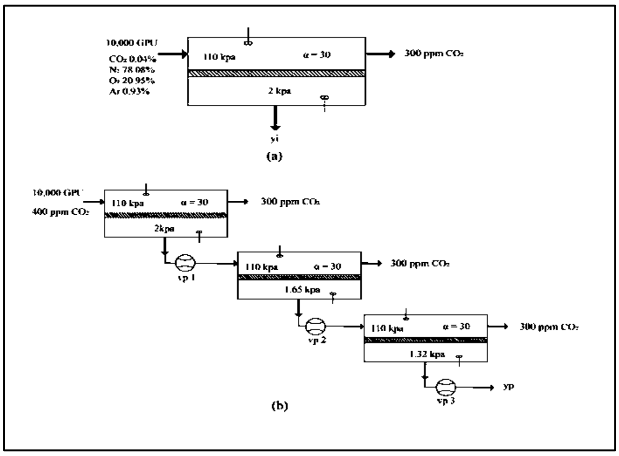

Figure (5): Process Flow Diagram for Complete Mixing Model 10,000 GPU, a) Multicomponent System Single Stage, b) Binary System Multistage.

In the second set of conditions, presented in Table (5), adjustments were made to the pressure and CO_2 permeance. However, it is important to note that the feed and outlet mole fractions of CO_2 remained unchanged.

Table (6): The Results of Permeate Mole Fraction and Area for Multicomponent System

comp	x_f	y_i	x_o
CO_2	0.00040	0.00587	0.0003
N_2	0.7808	0.776526	0.780878
O_2	0.20950	0.20835	0.209521
Ar	0.0093	0.009249	0.009301
sum	1.00000	1.00000	1.00000

θ	y_p	q_p (m^3/s)	A_m (m^2)	R_c
0.01795	0.00587	0.017949	66.10081	0.263462

Table (7): Vacuum Pump Required Energy for Multicomponent

γ (20 C)	1.4
R (J/gmol. k)	8.314
T (k)	298
E_{vacuum} (KJ)	3164.009
W_{min} (KJ)	-9.92846

Table (8): Permeate Mole Fraction of CO_2 and Membrane Area for Binary System Multistage

stage	1	2	3
p_l (kpa)	2	1.65	1.32
r (p_l/p_h)	0.018182	0.015	0.012
y_p	0.00593	0.00625	0.00665
θ	0.01776	0.946	0.937
A_m (m^2)	66.4	61.7	57.6
E_{vacuum} (KJ)	3021.986	3107.659	3198.852

Comparing the second condition to the first condition, several observations can be made. In the second condition, the CO_2 permeance is decreased to 10,000, resulting in a higher required membrane area of 66 m^2 and a decreased selectivity of 30. This can be interpreted as a lower permeance membrane allowing fewer CO_2 molecules to pass through, necessitating a larger area to maintain the desired outlet CO_2 concentration in the retentate side. Despite the lower pressure ratio, the required area is higher, indicating that permeance has a more significant impact on area requirements compared to the pressure ratio. It is worth noting the higher pumping energy required in this condition due to the lower pressure ratio. Additionally, in this condition, the feed pressure P(atm) is 110 kPa.

In the binary system CO_2/N_2 separation, three key findings emerge from the results. Firstly, the area decreases over stages due to the decreasing pressure ratio. Secondly, the vacuum pumping energy required decreases along the stages (as shown in Table (4)) because subsequent separation stages consume less energy since the gas volume is significantly reduced after the first stage. Although the reduced pressure ratio requires more energy (as observed in the second condition in Table (8)), this effect can offset the increased permeate mole fraction and reduced gas volume. Thirdly, the permeate mole fraction increases with each stage as the pressure ratio decreases. The purity of carbon dioxide is dependent on the utilization of the CO_2 product.

3.3 General Parameters Relations: Permeate Mole Fraction, Stage Cut, Pressure Ratio, Membrane Area, Permeance and Selectivity.

Regarding the general relations derived from the results, let's examine the permeate mole fraction of CO_2 and the stage cut illustrated in Figure (6). The stage cut represents the proportion of the feed that is directed to the permeate stream. The findings clearly indicate that as the stage cut increases, the permeate mole fraction decreases. This implies that a larger fraction of the feed is directed to the permeate stream, leading to a reduced concentration of the target gas in the permeate.

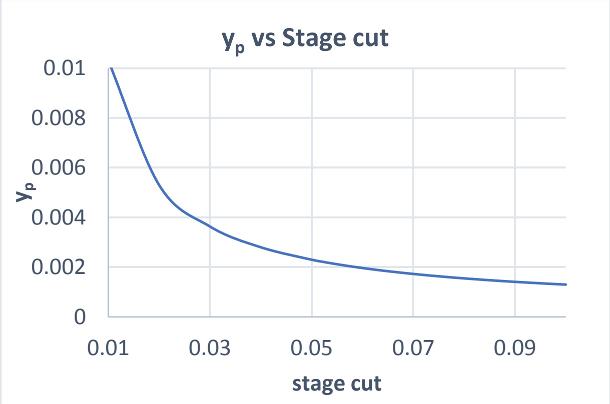

Figure (6): Carbon Dioxide Mole Fraction Relation with Stage cut.

The pressure ratio refers to the ratio of the permeate pressure to the feed pressure. In terms of membrane area, Figure (7) demonstrates that as the pressure ratio decreases, the required membrane area decreases for a given permeate flow rate. This reduction occurs because a lower pressure ratio results in a higher driving force for permeation, thereby requiring less membrane area to achieve the desired permeate flow rate. However, it is crucial to note that membrane area is also influenced by other factors such as selectivity, permeance, and stage cut.

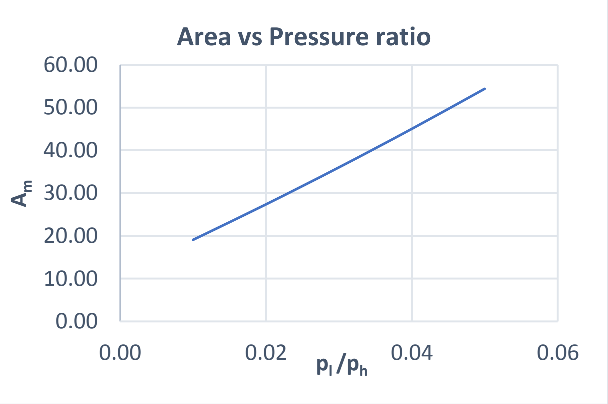

Figure (7): Membrane Area's Relation with Pressure Ratio

Determining the optimal pressure ratio depends on the trade-off with pumping energy requirements. Generally, a lower pressure ratio leads to a lower required membrane area but an increased demand for pumping energy. This concept is further supported by the findings in the second condition.

Figure (8) depicts the correlation between the permeate mole fraction and the pressure ratio, demonstrating a consistent decline in the mole fraction as the pressure ratio increases. This observation aligns with the assertion that an increase in the pressure ratio leads to a decrease in permeate purity [6]. The reason behind this trend is that a higher-pressure ratio reduces the driving force for gas permeation through the membrane, resulting in a lower flux and consequently a lower permeate mole fraction.

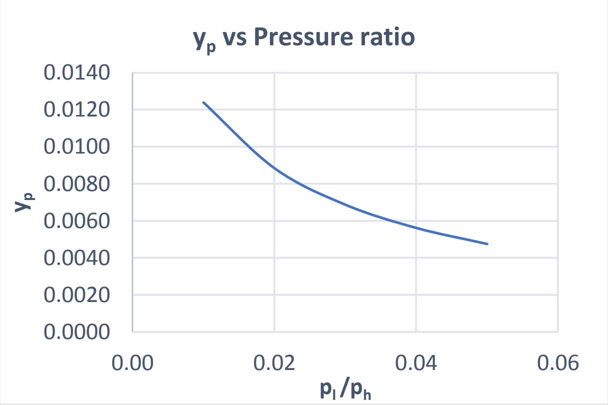

Figure (8): CO_2 Permeate Mole Fraction with Pressure Ratio.

Permeance is a crucial factor that significantly influences membrane performance. The findings presented in Figure (9) indicate that higher permeance values correspond to lower membrane area requirements for separation. This phenomenon occurs because higher permeance leads to increased flux, enabling greater separation efficiency to be achieved with a smaller membrane area.

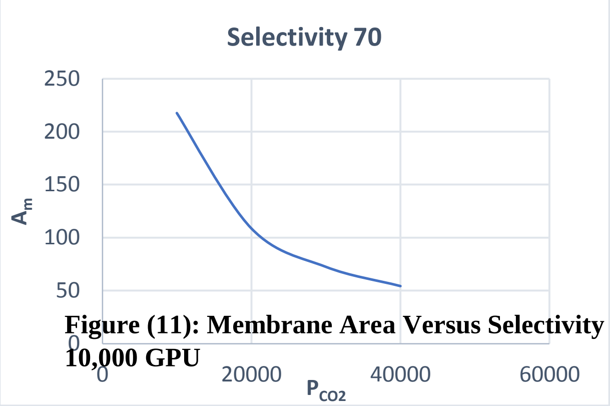

Figure (11): Membrane Area Versus Selectivity at 10,000 GPU

Figure (10) demonstrates that as the selectivity of the membrane increases, the separation performance of the membrane improves, leading to a higher permeate mole fraction of the desired component. This improvement occurs because the membrane becomes more effective at differentiating between the various components in the feed stream, allowing only the desired component to permeate through. Therefore, as a general trend, when the selectivity of a membrane increases, the permeate mole fraction of the desired component also increases, indicating enhanced separation performance of the membrane.

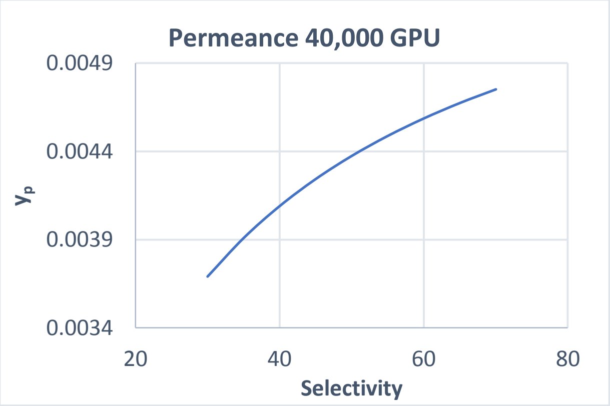

Figure (10): Carbon Dioxide Permeate Mole Fraction vs Selectivity at 40,000 GPU

The membrane area necessary for gas separation plays a crucial role in determining the overall cost and efficiency of the process. The findings depicted in Figure (11) indicate that, with a constant CO_2 permeance value of 10,000, the required membrane area for separation increases as the selectivity between the two gases rises. This outcome stems from the fact that selectivity dictates the amount of feed gas that must undergo processing to attain the desired level of separation. In systems with higher selectivity, a greater portion of the feed gas must be treated to remove a specific impurity quantity. Consequently, a larger membrane area is necessary to achieve an equivalent level of separation compared to systems with lower selectivity.

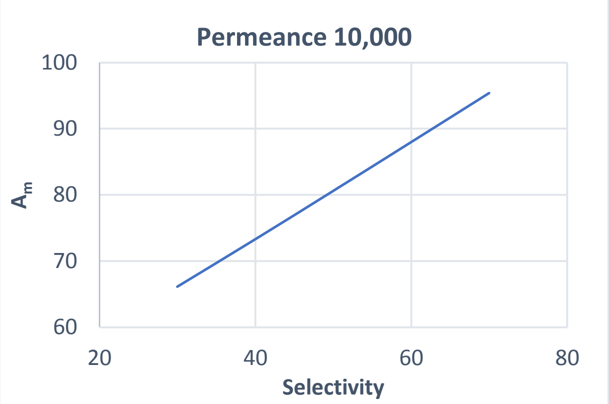

Figure (9): Membrane Area versus Carbon Dioxide Permeance at Selectivity of 70

Table (9) provides several examples of polymeric membrane materials along with their corresponding CO_2 permeance and CO_2/N_2 selectivity performances, sourced from [6]. Additionally, estimated values for stage cut, permeate mole fraction, and membrane area are included, assuming a complete mixing model. The selection of a suitable membrane material depends on factors such as cost and the specific application of the membrane system.

Table (9): Stage cut, Permeate Mole fraction and the Area of Different Membrane Materials.

Membrane material	θ	y_p	q_p (m^3/s)	A_m (m^2)
Poly[bis(2-2(methoxyethoxy)ethoxy)]phosphazene	0.02309	0.004631	0.02309	7980.82
Polyactive	0.024268	0.004421	0.024268	1586.44
Polaris	0.029499	0.00369	0.029499	612.37
PIM-1	0.032024	0.003423	0.032024	481.86
Polytrimethylsilylpropyne	0.053594	0.002166	0.053594	27.41

When comparing the permeate mole fraction calculated using the perfect mixing and crossflow model in Table(10), the findings indicate that the crossflow model predicts a slightly higher permeate mole fraction than the perfect mixing model. This disparity arises due to the fact that the crossflow model takes into account concentration polarization and the resulting concentration gradients across the membrane. These factors contribute to an increased permeate flux, resulting in a higher permeate mole fraction (y_p).

Table (10): Crossflow Weller and Steiner Analytical Solution Results for Permeate Mole Fraction and Stage Cut at 40,000 GPU and 70 Selectivity Conditions.

D	F	E	R	S	T	i_f	u_f
33.29208	2.207921	-38.5063	0.015248	1.052083	-0.06733	0.0004	2.187649
x	i	u	θ*	y_p			
0.0003	0.0003	2.192713	0.019207	0.005506			

Polymath Program for Solving the Cross Flow Model for Binary System

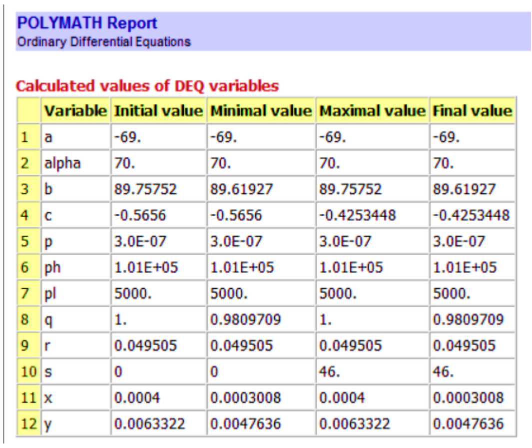

POLYMATH Report
Ordinary Differential Equations

Calculated values of DEQ variables

	Variable	Initial value	Minimal value	Maximal value	Final value
1	a	-69.	-69.	-69.	-69.
2	alpha	70.	70.	70.	70.
3	b	89.75752	89.61927	89.75752	89.61927
4	c	-0.5656	-0.5656	-0.4253448	-0.4253448
5	p	3.0E-07	3.0E-07	3.0E-07	3.0E-07
6	ph	1.01E+05	1.01E+05	1.01E+05	1.01E+05
7	pl	5000.	5000.	5000.	5000.
8	q	1.	0.9809709	1.	0.9809709
9	r	0.049505	0.049505	0.049505	0.049505
10	s	0	0	46.	46.
11	x	0.0004	0.0003008	0.0004	0.0003008
12	y	0.0063322	0.0047636	0.0063322	0.0047636

Figure (12): Polymath Report and Code for Cross Flow Model in the First Condition.

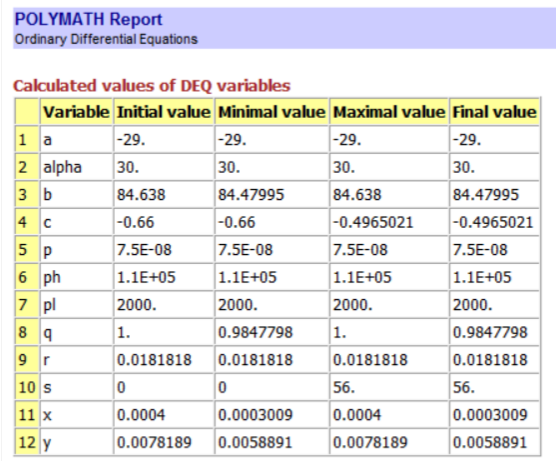

POLYMATH Report
Ordinary Differential Equations

Calculated values of DEQ variables

	Variable	Initial value	Minimal value	Maximal value	Final value
1	a	-29.	-29.	-29.	-29.
2	alpha	30.	30.	30.	30.
3	b	84.638	84.47995	84.638	84.47995
4	c	-0.66	-0.66	-0.4965021	-0.4965021
5	p	7.5E-08	7.5E-08	7.5E-08	7.5E-08
6	ph	1.1E+05	1.1E+05	1.1E+05	1.1E+05
7	pl	2000.	2000.	2000.	2000.
8	q	1.	0.9847798	1.	0.9847798
9	r	0.0181818	0.0181818	0.0181818	0.0181818
10	s	0	0	56.	56.
11	x	0.0004	0.0003009	0.0004	0.0003009
12	y	0.0078189	0.0058891	0.0078189	0.0058891

Figure (13): Polymath Report and Code for Cross Flow Model in the Second Condition.

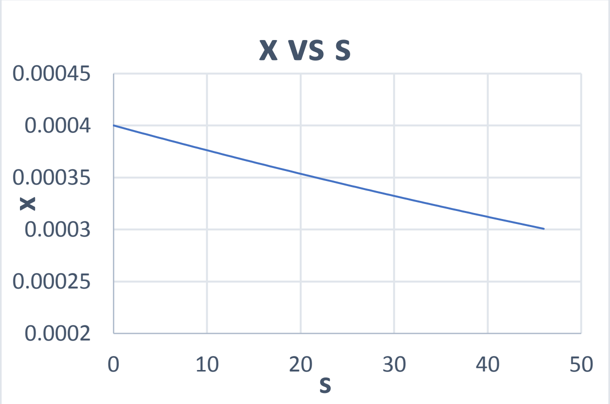

Figure (14): CO_2 Mole Fraction Against Area in Upstream (x vs s) For Cross Flow Case, First Condition.

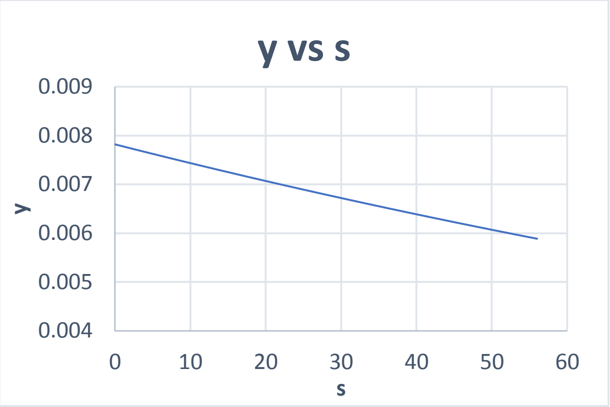

Figure (15): CO_2 Mole Fraction Against Area in Downstream or Permeate Side (y vs s) for Cross Flow Case, Second Condition.

The estimated membrane area, obtained using the Polymath program, for the two conditions depicted in Figure (12) and Figure (13), was 46 m^2 and 56 m^2, respectively. Figure (14) and Figure (15) illustrate the relationship between the carbon dioxide concentration in the upstream and downstream regions and the membrane area S, which exhibits an inverse proportionality.

Collectively, these results emphasize the significance of considering factors such as membrane area, permeance, stage cut, pressure ratio, and the chosen modeling approach when designing a membrane gas separation process. The findings suggest that the complete mixing flow model serves as a suitable representation for achieving high purity, low stage cut, and recovery in the DAC (Direct Air Capture) process. However, it is important to note that one limitation of this study is the absence of other flow cases, such as Cross Flow, which, if examined for multicomponent scenarios, could provide a more detailed understanding of the permeation of CO_2 and other air components within the membrane.

CONCLUSIONS AND RECOMMENDATIONS

The objective of this study was to explore the separation performance of a single and multistage membrane module for Direct Air Capture (DAC) of carbon dioxide. A parametric engineering study was conducted, employing various membrane materials and operating conditions. The results revealed that there was minimal difference in performance between multicomponent and binary systems in DAC for carbon dioxide separation.

In the binary system focused on CO_2/N_2 separation, several key findings were identified. These included a reduction in membrane area over stages, changes in vacuum pumping energy requirements, and an increase in permeate mole fraction along the stages with decreasing pressure ratio. The study also highlighted the critical role of membrane area as a parameter that significantly impacts the overall cost and efficiency of the process.

However, it is important to note that the study had a limitation in that it did not investigate the impact of wet air compounds on the separation process. Considering the potential presence of these compounds could be crucial, particularly for specific applications of the captured CO_2.

Planting trees and incentivizing sustainable forest products combat climate change. In order to meet the IPCC's recommended goal of limiting global warming to 1.5°C, alternative approaches to carbon capture must be explored. Membrane separation is a promising and scalable technique for carbon capture that doesn't require special chemicals or sorbents and is suitable for small-scale systems. Future research could explore water vapor effects, conduct an economic evaluation, and compare membrane and sorbent DAC technologies for wider adoption. Additionally, investigating other flow cases and optimizing the process can help pave the way for more efficient and large-scale implementation of DAC.

REFERENCES

Astro-Munoz R., M. Zamidi, M. Malankowska, and J. Coronas, "A New Relevant Membrane Application: CO_2 Direct Air Capture (DAC)", Chemical Engineering Journal, 442 (2022).

Bounaceur R., E. Berger, M. Pfister, A. Andres, R. Santos and E. Favre, "Rigorous Variable Permeability Modelling and Process Simulation for the Design of Polymeric Membrane Gas Separation Units: MEMSIC Simulation Tool", Journal of Membrane Science, 523 (2017), P.P. 77-91.

Castel C., R. Bounaceur and E. Favre, "Membrane Processes for Direct Carbon Dioxide Capture from Air: Possibilities and Limitations", Frontiers in Chemical Engineering, 3 (2021).

Cengel Y. A., "Introduction to Thermodynamics and Heat Transfer", 2nd Edition, (2008).

Fujikawa S., R. Selyanchyn, and T. Kunitake, "A New Strategy for Membrane Based Direct Air Capture", Polymer Journal, 53 (2021), P.P. 111-119.

Geankoplis C. J., "Transport Processes and Unit Operations", 3rd Edition, (1993).

Sandalow, D., J. Friedmann, C. McCormick, and S. McCoy, "Direct Air Capture of Carbon Dioxide", ICEF Roadmap (2018). Retrieved from ICEF Roadmap (2018): Direct Air Capture of Carbon Dioxide - Global CCS Institute

https://climate.nasa.gov/news/2915/the-atmosphere-getting-a-handle-on-carbon-dioxide//

Smith J. M., H. C. Van Ness, and M. M. Abbott, "Introduction to Chemical Engineering Thermodynamics", 7th Edition, (2005).